

Dietary and Genetic Control of Glucose Transporter 2 Glycosylation Promotes Insulin Secretion in Suppressing Diabetes

Kazuaki Ohtsubo,¹ Shinji Takamatsu,^{2,3} Mari T. Minowa,² Aruto Yoshida,² Makoto Takeuchi,² and Jamey D. Marth^{1,*}

¹Howard Hughes Medical Institute and Department of Cellular and Molecular Medicine, 9500 Gilman Drive, University of California, San Diego, La Jolla, CA 92093, USA

²Central Laboratories for Key Technology, Kirin Brewery Co. Ltd., 1-13-5 Fuku-ura, Kanazawa-ku, Yokohama, Kanagawa 236-0004, Japan

³Biomedical Imaging Research Center, University of Fukui, 23-3 Shimoaizuki, Matsuoka, Yoshida, Fukui 910-1193, Japan

*Contact: jmarth@ucsd.edu

DOI 10.1016/j.cell.2005.09.041

SUMMARY

Pancreatic β cell-surface expression of glucose transporter 2 (Glut-2) is essential for glucose-stimulated insulin secretion, thereby controlling blood glucose homeostasis in response to dietary intake. We show that the murine GlcNAcT-IVa glycosyltransferase is required for Glut-2 residency on the β cell surface by constructing a cell-type- and glycoprotein-specific N-glycan ligand for pancreatic lectin receptors. Loss of GlcNAcT-IVa, or the addition of glycan ligand mimetics, attenuates Glut-2 cell-surface half-life, provoking endocytosis with redistribution into endosomes and lysosomes. The ensuing impairment of glucose-stimulated insulin secretion leads to metabolic dysfunction diagnostic of type 2 diabetes. Remarkably, the induction of diabetes by chronic ingestion of a high-fat diet is associated with reduced GlcNAcT-IV expression and attenuated Glut-2 glycosylation coincident with Glut-2 endocytosis. We infer that β cell glucose-transporter glycosylation mediates a link between diet and insulin production that typically suppresses the pathogenesis of type 2 diabetes.

INTRODUCTION

Glucose transporters (Gluts) are a family of integral membrane glycoproteins that transport saccharides across the cell plasma membrane by facilitative diffusion to supply met-

abolic energy (Olson and Pessin, 1996; Joost and Thorens, 2001). Glut family members have different expression patterns, and their abundance can change in response to altered metabolic states. Induced Glut expression is observed in some cancers, perhaps reflecting the need for increased glycolysis in supporting unrestrained cell growth (Macheda et al., 2005), while decrements in Glut transporter function can be pathogenic markers of other disorders. Loss of pancreatic β cell Glut expression in humans and rodents is associated with hyperglycemia and diminished glucose-stimulated insulin secretion (GSIS), which are early markers in the pathogenesis of diabetes and precede the development of insulin resistance (Johnson et al., 1990; Orci et al., 1990a; Thorens et al., 1990; Unger, 1991; Guerra et al., 2005). Glut-2 is essential for the primary GSIS response of mouse β cells, and reduced Glut-2 expression abolishes this role of the pancreas coincident with the onset of type 2 diabetes (Valera et al., 1994; Guillam et al., 1997, 2000).

Diminished β cell-surface Glut-2 expression has been observed with intracellular accumulation among mice fed a high-fat diet and β cells exposed to increased glucocorticoid levels, implying the presence of a posttranslational mechanism that modulates Glut-2 trafficking (Gremlich et al., 1997; Reimer and Ahren, 2002). Remarkably, all vertebrate glucose transporters bear a single conserved N-glycosylation consensus site that is typically positioned in the first or fifth extracellular loop (Joost and Thorens, 2001). Glut-2 is N-glycosylated in the endoplasmic reticulum and Golgi apparatus prior to being trafficked to the cell surface by the constitutive pathway and does not normally reside among intracellular vesicles (Thorens et al., 1993). N-glycosylation may be involved in modulating Glut function, however, as altered intracellular trafficking and glucose-transport kinetics have been observed among Glut-1 and Glut-4 molecules engineered to lack N-glycosylation consensus sites (Asano et al., 1993; Ing et al., 1996).

Glycan structures found on secreted and cell-surface glycoproteins such as the glucose transporters may be branched multiantennary complex types, which are among

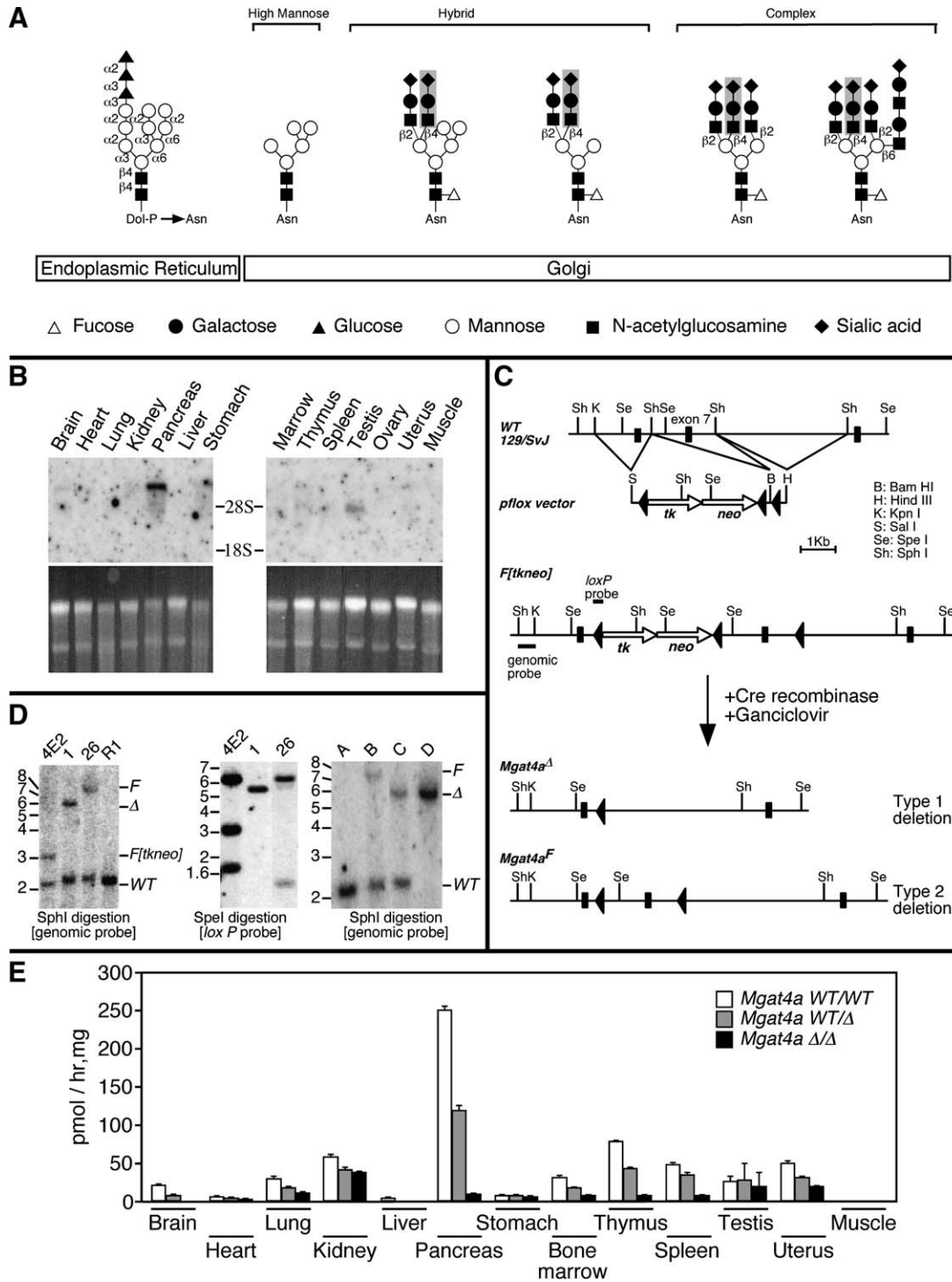


Figure 1. Activity, Expression, and Mutagenesis of the *Mgat4a*-Encoded GnT-4a Glycosyltransferase

(A) Mammalian protein N-glycosylation begins in the endoplasmic reticulum and proceeds in the Golgi apparatus, where three types of mature N-glycan structures are produced—high-mannose, hybrid, and complex types. The GnT-4a glycosyltransferase transfers N-acetylglucosamine in β 4 linkage to underlying α 3-linked mannose, thereby initiating formation of this distinct N-glycan branch exemplified as a sialylated N-acetylglucosamine sequence (shaded). (B) Expression of mouse *Mgat4a* RNA transcripts among total RNA samples from indicated tissues ($n = 6$). (C) Mouse genomic clone of *Mgat4a* bearing exons 6, 7, and 8 (black boxes) used for constructing the targeting vector with the *plox* plasmid as indicated. Homologous recombination produces the *Mgat4a* F[tk-neo] allele. Following Cre recombination and selection, embryonic stem (ES) cell clones are isolated containing the type 1 (Δ , deleted) and type 2 (F, floxed) alleles.

the most prevalent of mature N-glycan forms (Figure 1A). Precisely which glycan branches and which linkages are present is determined by glycosyltransferase expression patterns and their encoded substrate specificities, making this enzyme family an attractive target for genetic investigations of the function of protein glycosylation (Lowe and Marth, 2003). The *Mgat4a*-encoded GlcNAcT-IV glycosyltransferase (herein referred to as GnT-4a) is one of two isozymes that synthesize the β 4 N-acetylglucosamine linkage on the α 3-linked mannose, thus initiating the formation of this distinct N-glycan branch (Minowa et al., 1998; Yoshida et al., 1998; Figure 1A). We observed that the mouse *Mgat4a* gene is selectively expressed among normal tissues, with high levels in the pancreas (Figure 1B).

We have further examined the physiologic role of GnT-4a activity and the N-glycan branch structure it produces by engineering and characterizing mice lacking *Mgat4a* gene function. We find that GnT-4a is essential for the production of a complex-type glycan ligand on the pancreatic β cell Glut-2 glycoprotein that stabilizes Glut-2 cell-surface expression by a lectin-receptor binding mechanism. Dietary and genetic disruption of this mechanism results in Glut-2 endocytosis, loss of the first phase of GSIS, and the pathogenesis of type 2 diabetes.

RESULTS

Mutagenesis of the *Mgat4a* Gene Encoding the GnT-4a Glycosyltransferase

Elimination of GnT-4a activity from the mouse germline was initiated by conditional mutagenesis of the *Mgat4a* allele using Cre-loxP recombination in embryonic stem (ES) cells (Figure 1C). Exon 7 of *Mgat4a* was flanked (F) by loxP sites (Figure 1D). Mice bearing the *Mgat4a^F* allele were bred with mates expressing the Cre recombinase in developing oocytes (Shafi et al., 2000) to produce offspring bearing the deleted (Δ) *Mgat4a^{\Delta}* allele lacking exon 7 (Figure 1D). All alleles were crossed into the C57BL/6 strain background for six or more generations prior to study. Mutant allele segregation among offspring was normal, and animals homozygous for either mutation lacked overt physical, neurologic, immunologic, or reproductive defects. Animals homozygous for the *Mgat4a^F* allele were indistinguishable from wild-type littermates in all studies undertaken below (data not shown).

Loss of exon 7 disrupts the GnT-4a catalytic domain and results in a frameshift followed closely by a translational termination signal (Minowa et al., 1998; data not shown). Among tissues surveyed, GnT-4 enzymatic activity was found to be high in the pancreas of wild-type mice (Figure 1E). Most tissues of mice heterozygous for the *Mgat4a^{\Delta}* allele expressed approximately 50% of wild-type GnT-4 ac-

tivity levels, while homozygote samples typically retained 2%–20%. Remaining GnT-4 activity is likely due to expression of the *Mgat4b*-encoded GnT-4b isozyme (Yoshida et al., 1998). We infer that deletion of exon 7 in the mouse *Mgat4a* gene eliminates GnT-4a activity.

GnT-4a Deficiency Impairs β Cell Glucose Transport and Insulin Secretion in Causing Type 2 Diabetes

Serological analyses of 8- to 12-week-old GnT-4a-deficient mice revealed elevated blood glucose concentrations (Table 1). Free fatty acid and triglyceride levels were also significantly increased, while serum insulin concentrations remained below normal. These abnormalities intensified as animals provided a standard chow diet ad libitum reached 1 year of age, while enzymatic markers of liver damage appeared during this time. By 6–8 months of age, GnT-4a-deficient mice gained 20% in body mass over that of wild-type littermates without a measurable increase in food intake. These results implied a possible defect in pancreatic function.

The pancreas of GnT-4a-deficient mice appeared unremarkable upon histologic analysis and were without evidence of leukocyte infiltrates (Figure 2A). The abundance and size of pancreatic islets were also normal (Figure 2B). However, GnT-4a-deficient mice exhibited an abnormal response in the glucose-tolerance test, yielding blood glucose levels that were substantially and persistently elevated (Figure 2C). Remarkably, insulin failed to significantly increase upon glucose challenge (Figure 2D). Insulin insufficiency was not due to a defect in insulin production or the secretory process in general as L-arginine injection produced a robust increase in serum insulin (Figure 2E). Although insulin sensitivity was normal at 8–12 weeks of age, insulin resistance was prevalent among GnT-4a-deficient animals by 1 year of age (Figures 2F and 2G). During this time, RNA levels encoding the liver gluconeogenic enzymes phosphoenolpyruvate carboxykinase and glucose-6-phosphatase remained elevated among GnT-4a-deficient mice (Figure 2H), while hepatic steatosis was pronounced by 6 months of age (Figure 2I). These metabolic alterations indicate that GnT-4a deficiency in the mouse causes failure of pancreatic β cell function to appropriately secrete insulin and evokes a phenotype diagnostic of type 2 diabetes.

Glucose-transport and insulin-secretion kinetics were investigated by in vitro perfusion among pancreatic islet cell cultures comprised of >90% β cells. GnT-4a-deficient islet cells failed to undergo the primary GSIS response and exhibited a reduced secondary insulin secretion response (Figure 2J). The kinetics of glucose transport by pancreatic islet cells were therefore investigated using the fluorescent analog 2-NBDG. Wild-type islet cells transported 2-NBDG

(D) Genomic Southern blotting confirmed the predicted *Mgat4a* allelic structures. Left and middle panels: ES cell clones bearing indicated mutant *Mgat4a* alleles in comparison with R1 parental wild-type ES cells. Right panel: adult mouse genotypes with germline modifications to the *Mgat4a* gene, including *Mgat4a^F* and *Mgat4a^{\Delta}* alleles.

(E) GnT-4a enzyme activity among genotypes and tissues surveyed. Results are expressed as mean \pm SD (n = 3).

Table 1. Serology and Body Weight

8–12 Weeks of Age, Standard Chow	Wild-Type (n = 20)	<i>Mgat4a</i> Null (n = 20)
Glucose (fasting) (mg/dl)	96.20 ± 6.26	137.05 ± 5.68 (p = 0.0001)
Glucose (fed) (mg/dl)	138.82 ± 6.55	193.59 ± 8.99 (p = 0.0001)
Insulin (fasting) (ng/ml)	0.712 ± 0.048	0.633 ± 0.036
Insulin (fed) (ng/ml)	2.916 ± 0.373	1.191 ± 0.105 (p = 0.0001)
Free fatty acid (fasting)	1.04 ± 0.04	1.360 ± 0.120 (p = 0.0361)
Free fatty acid (fed)	0.58 ± 0.06	0.58 ± 0.04
Triglyceride (mg/dl)	47.3 ± 2.02	91.70 ± 10.80 (p = 0.0002)
AST (IU/l)	76.36 ± 5.68	96.31 ± 11.83
ALT (IU/l)	24.92 ± 1.03	27.85 ± 1.55
Lipase (U/l)	48.33 ± 2.15	44.62 ± 1.75
Total cholesterol (mg/dl)	94.67 ± 4.76	105.12 ± 6.80
HDL cholesterol (mg/dl)	79.72 ± 5.56	88.94 ± 7.30
Body weight (g)	27.20 ± 1.40	29.60 ± 1.75
12 Months of Age, Standard Chow	Wild-Type (n = 15)	<i>Mgat4a</i> Null (n = 15)
Glucose (fasting) (mg/dl)	108.9 ± 7.72	168.6 ± 10.14 (p = 0.0001)
Glucose (fed) (mg/dl)	193.2 ± 8.12	249.4 ± 15.41 (p = 0.0029)
Insulin (fasting) (ng/ml)	1.023 ± 0.127	0.651 ± 0.087 (p = 0.0239)
Insulin (fed) (ng/ml)	4.389 ± 0.361	1.673 ± 0.121 (p = 0.0001)
Free fatty acid (fasting)	1.10 ± 0.03	1.660 ± 0.050 (p = 0.0001)
Free fatty acid (fed)	0.62 ± 0.06	0.680 ± 0.040
Triglyceride (mg/dl)	102.6 ± 8.93	158.5 ± 18.75 (p = 0.0174)
AST (IU/l)	96.52 ± 6.58	170.8 ± 14.21 (p = 0.0003)
ALT (IU/l)	87.39 ± 6.60	173.2 ± 10.57 (p = 0.0001)
Lipase (U/l)	60.63 ± 4.81	52.82 ± 3.80
Total cholesterol (mg/dl)	190.9 ± 15.00	176.6 ± 14.32
HDL cholesterol (mg/dl)	168.0 ± 7.84	152.0 ± 12.57
Body weight (g)	47.98 ± 1.92	57.98 ± 2.27 (p = 0.0031)
12 Weeks of Age, 8 Weeks on High-Fat Chow	Wild-Type (n = 14)	<i>Mgat4a</i> Null (n = 14)
Glucose (fasting) (mg/dl)	214.5 ± 21.25	208.9 ± 8.91
Glucose (fed) (mg/dl)	237.4 ± 11.53	307.2 ± 10.45 (p = 0.0001)
Insulin (fasting) (ng/ml)	5.838 ± 1.313	2.656 ± 0.551 (p = 0.0423)
Insulin (fed) (ng/ml)	6.617 ± 0.907	4.023 ± 0.324 (p = 0.0123)
Free fatty acid (fasting)	1.85 ± 0.09	1.780 ± 0.060
Free fatty acid (fed)	1.59 ± 0.08	1.560 ± 0.060
Triglyceride (mg/dl)	104.3 ± 8.53	98.86 ± 5.53
AST (IU/l)	100.9 ± 7.19	106.0 ± 5.62
ALT (IU/l)	72.50 ± 9.31	84.29 ± 6.87
Lipase (U/l)	64.50 ± 6.70	66.00 ± 7.27
Total cholesterol (mg/dl)	149.2 ± 10.80	171.1 ± 4.70
HDL cholesterol (mg/dl)	122.0 ± 8.49	117.9 ± 5.96
Body weight (g)	39.00 ± 1.90	47.17 ± 2.47 (p = 0.0002)

across the plasma membrane in a glucose-dependent manner at the nominal rate, while 2-NBDG uptake in GnT-4a-deficient cells was significantly reduced (Figure 2K). The K_d of 2-NBDG binding at the cell surface was not altered; in contrast, a 9-fold decrease in V_{max} occurred in GnT-4a deficiency (Figure 2L). These findings suggested normal glucose-transporter function in the absence of GnT-4a and were consistent with reduced glucose-transporter expression.

Intracellular Glut-2 Localization in GnT-4a Deficiency

The in situ expression of β cell Glut-2 glycoprotein was analyzed by fluorescent deconvolution microscopy using immunological markers of intracellular compartments. Glut-2 glycoprotein trafficking was profoundly altered by GnT-4a deficiency. Normally, Glut-2 is disbursed on the β cell plasma membrane, in contrast to the predominantly intracellular punctate expression observed in GnT-4a deficiency (Figures 3A and 3B). Colocalization analysis indicated no major overlap with insulin secretory vesicles, the endoplasmic reticulum, the *cis*-Golgi, or the *trans*-Golgi (Figures 3A–3P). In contrast, Glut-2 glycoprotein accumulation was significantly increased in endosomes and lysosomes (Figures 3Q–3X). These results imply that the β cell Glut-2 N-glycan plays a role in promoting cell-surface expression of the Glut-2 glycoprotein.

Structure and Specificity of N-Glycans Promoting β Cell-surface Expression of Glut-2

The Glut-2 protein sequence is highly conserved among vertebrates, including a single N-glycosylation site in the first extracellular loop (Figure 4A). In addition to the intracellular accumulation of β cell Glut-2 in the absence of glycosylation by GnT-4a, a significant reduction in total islet-cell Glut-2 glycoprotein level was observed (Figure 4B). This was associated with Glut-2 N-glycan structural changes detected by plant lectin binding (reviewed in Cummings, 1999). A reduction in binding of the DSL lectin to remaining Glut-2 in *Mgat4a* null islet cells indicated loss of the N-glycan branch normally formed by Golgi GnT-4 activity (Figure 4B). Additional results with LEA, ECA, RCA, SNA, and MAH lectins implied the absence of poly-lactosamine and terminal sialic acids, along with the presence of terminal galactose linkages that comprise Glut-2 N-glycan structures from both genotypes. Unexpectedly, the N-glycan branch contributed by Golgi GnT-5 activity and visualized by L-PHA lectin binding was also absent from the Glut-2 N-glycan in GnT-4a deficiency. We therefore analyzed islet-cell Glut-2 abundance and glycan structure among *Mgat5* null mice lacking GnT-5 activity (Demetriou et al., 2001). Glycan ligands of L-PHA were deficient as expected, while no alteration in Glut-2 abundance or DSL binding was observed (Figure 4C).

The N-glycan structure of pancreatic Glut-2 from wild-type mice inferred from plant lectin binding profiles is a tetra-antennary complex type bearing little or no sialic acid and instead containing terminal galactose residues linked to underlying N-acetylglucosamine (LacNAc) (Figure 4D, left). Absence of GnT-4a results in a biantennary-complex-type

N-glycan, while GnT-5 deficiency engenders a triantennary-complex-type structure (Figure 4D, middle and right). Changes to islet-cell N-glycans in GnT-4a deficiency were not limited to Glut-2. Loss of GnT-4a activity similarly altered N-glycan structures on other glycoproteins, including the insulin receptor α subunit and insulin-like growth factor 1 receptor. Expression levels of these glycoproteins were nevertheless unaffected by GnT-4a deficiency (Figure 4E and data not shown).

Intact and membrane-permeable conditions were used in flow cytometric analyses to separately measure cell-surface and total glycoprotein expression, respectively, among pancreatic islet cells. Cell-surface and total Glut-2 glycoprotein levels closely overlapped among wild-type cells. In GnT-4a deficiency, Glut-2 cell-surface expression was reduced to 15% of normal, while a 40% loss of total cellular Glut-2 glycoprotein was indicated (Figure 4F). *Mgat5* null islet cells retained normal Glut-2 expression profiles, and these animals did not exhibit hyperglycemia (Figure 4F and data not shown). Remarkably, none of these genetic lesions in N-glycan branching disrupted cell-surface localization of misglycosylated insulin receptor α or insulin-like growth factor 1 receptor (Figure 4F and data not shown). In addition, islet cells heterozygous for the *Mgat4a*^d allele exhibited an intermediate phenotype, implying that altered GnT-4a expression may in some contexts limit the extent of Glut-2 glycosylation and cell-surface abundance. We therefore evaluated *Mgat4a* RNA levels and Glut-2 glycosylation in response to an altered diet.

Attenuation of GnT-4a and Glut-2 by the High-Fat Diet

Administration of a high-fat diet to mice of the C57BL/6 strain diminishes pancreatic β cell Glut-2 expression coincident with increased intracellular accumulation, resulting in hyperglycemia and loss of GSIS early in the development of type 2 diabetes (Lee et al., 1995; Surwit et al., 1988; Reimer and Ahren, 2002; Winzell and Ahren, 2004). Serological findings of both wild-type and GnT-4a-deficient littermates receiving the high-fat diet for 8 weeks were consistent with diabetes (Table 1). GnT-4a deficiency exacerbated the hyperglycemia, moderately reduced the hyperinsulinemia, and increased body weight as compared to wild-type littermates. Otherwise, diabetic disease signs were similar among mice of both genotypes.

Littermates receiving the standard chow diet exhibited robust Glut-2 protein expression predominantly at the cell surface (Figures 5A, 5E, and 5I). In contrast, β cells from mice receiving a high-fat diet expressed markedly diminished cell-surface Glut-2 levels coincident with intracellular accumulation (Figures 5B, 5F, and 5J). Colocalization analyses using antibodies to intracellular markers revealed that the high-fat diet induced Glut-2 accumulation in early endosomes and lysosomes (Figures 5C, 5D, 5G, 5H, 5K, and 5L), replicating results obtained among GnT-4a-deficient mice receiving the standard chow diet.

Coincident with Glut-2 endocytosis, the high-fat diet attenuated *Mgat4a* RNA levels by 4-fold in comparison to littermates maintained on the standard chow diet (Figure 5M).

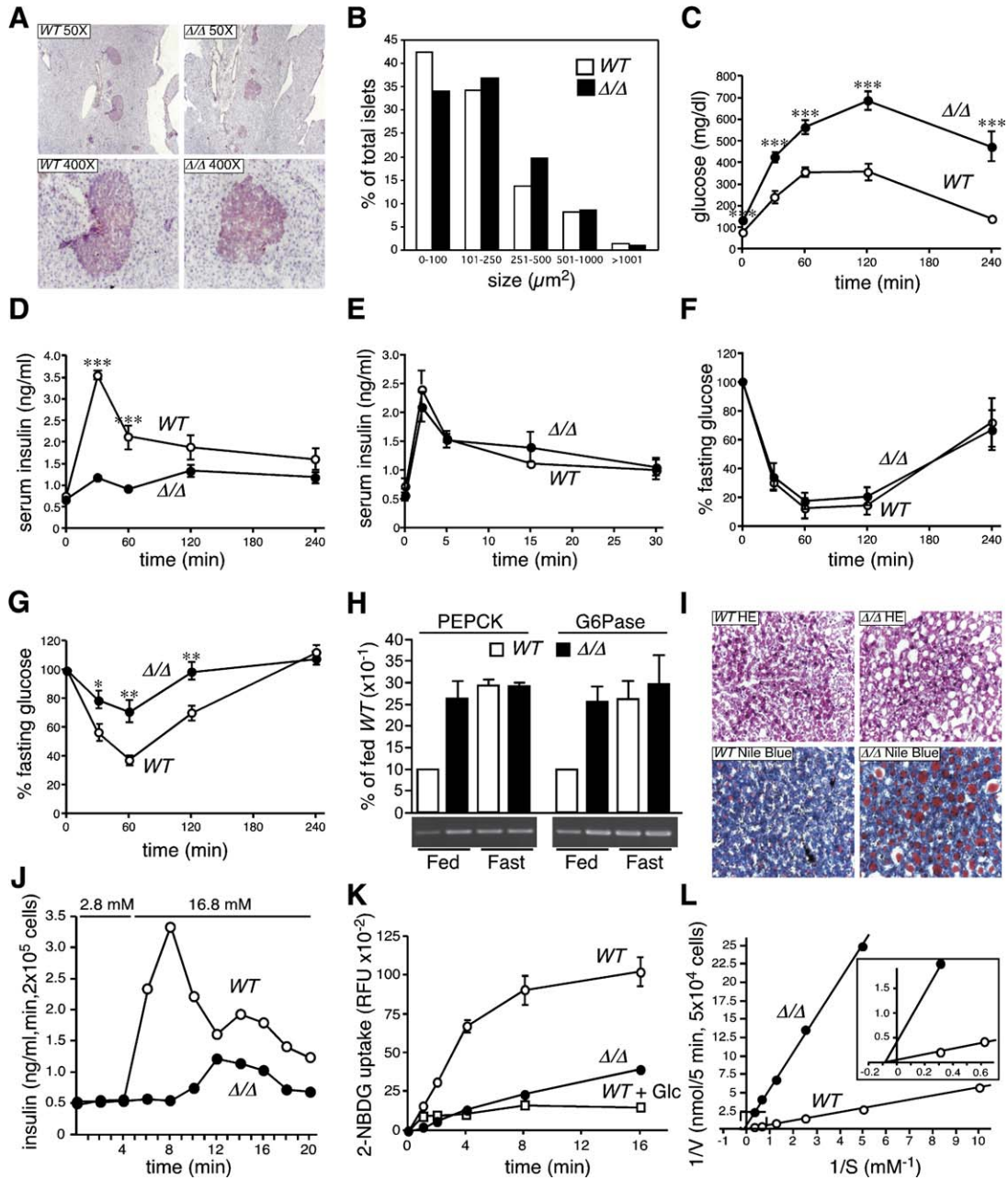


Figure 2. Type 2 Diabetic Phenotype of Gnt-4a-Deficient Mice Associated with Reduced Pancreatic Islet Cell Glucose Uptake and Diminished Insulin Secretion

(A) Insulin visualized (red) with HRP-conjugated secondary antibody in pancreatic sections of wild-type and Gnt-4a-deficient mice counterstained with hematoxylin.

(B) The size and distribution of pancreatic islets among littermates. Wild-type and *Mgat4a* null islets averaged $211.74 \pm 29.06 \text{ mm}^2$ and $234.03 \pm 24.22 \text{ mm}^2$, respectively ($n = 6$).

(C) Glucose-tolerance test comparing fasted wild-type (white circles) and *Mgat4a* null (black circles) littermates ($n = 10$; $***p < 0.0001$).

(D) Serum insulin levels measured during the glucose tolerance test ($n = 10$; $***p < 0.0001$).

(E) Insulin in circulation following L-arginine injection ($n = 10$).

(F and G) Serum glucose levels in mice fasted for 5 hr following insulin injection. Data are graphed as the percent of blood glucose levels pre-insulin treatment in wild-type (white circles) and *Mgat4a* null (black circles) littermates. Mice ($n = 10$) were aged either 12 weeks (F) or 1 year (G) ($**p < 0.001$; $*p < 0.005$). In (C)–(G), results are plotted as mean \pm SEM.

(H) PEPCK and G6Pase RNA levels measured in total RNA samples from liver tissue as a percent of fed 6-month-old wild-type littermate values.

(I) Liver tissue sections from 6-month-old littermates stained with hematoxylin and eosin (HE). Lipids were visualized using Nile blue (red). Magnification 200 \times .

Remarkably, impaired Glut-2 glycosylation by GnT-4a was also evident among animals receiving the high-fat diet (Figure 5N). These findings reveal that GnT-4a expression and Glut-2 glycosylation are under dietary regulation and imply that loss of β cell-surface Glut-2 in response to the high-fat diet may be a consequence of diminished GnT-4a activity.

Glut-2 Glycosylation Mediates β Cell-Surface Retention by a Lectin Binding Mechanism

Decreased cell-surface Glut-2 expression in GnT-4a deficiency may arise from a defect in trafficking from the Golgi apparatus to the cell surface or perhaps from a reduction in cell-surface half-life. The kinetics of Glut-2 synthesis and cell-surface appearance were measured among pancreatic islet cells derived from mice fed a standard chow diet using metabolic labeling coupled with cell-surface biotinylation. Glut-2 synthesis and trafficking to the cell surface takes 50–60 min in wild-type pancreatic islet cells. This was not altered by GnT-4a deficiency (Figure 6A). In contrast, Glut-2 half-life at the cell surface in the absence of GnT-4a was decreased by more than 4-fold (Figure 6B). GnT-4a glycosylation therefore increases Glut-2 cell-surface half-life, implying the possibility of a lectin binding interaction involving the Glut-2 N-glycan structure.

To detect the presence of a lectin receptor, we incubated pancreatic islet cell cultures established from wild-type mice fed a standard chow diet with synthetic glycan structures that included those present on Glut-2 N-glycan branches at concentrations typical within the region of the cell-surface glycocalyx. A profound reduction of cell-surface Glut-2 expression was observed within 2 hr after the addition of synthetic LacNAc (Gal β 1-4GlcNAc) containing glycans to islet cell cultures without loss of cell viability (Figure 6C). Increasing the number of LacNAc repeats enhanced this effect, while no significant reduction of cell-surface Glut-2 occurred using sucrose (Fru-Glc) or LacNAc bearing terminal sialic acid linkages. While these results may reflect alterations in multiple cell processes, they are consistent with competitive inhibition of lectin-receptor binding for nonsialylated LacNAc structures present within the Glut-2 N-glycan.

Lectins that bind nonsialylated LacNAc sequences include the family of galectins (Cooper and Barondes, 1999). Galectin-9 is also a urate transporter (UAT) and exhibits glycan binding selectivity for LacNAc-bearing sequences (Sato et al., 2002; Lipkowitz et al., 2004). Colocalization of Glut-2 and Galectin-9/UAT was detected in situ by fluorescent deconvolution microscopy among wild-type β cells of pancreatic tissues and was quantifiably reduced among GnT-4a-deficient β cells, reflecting diminished Glut-2 cell-surface

expression (Figure 6D). Cell-surface protein crosslinking and subsequent coprecipitation further indicated that Glut-2 and Galectin-9/UAT are normally in close proximity on the cell surface (Figure 6E). Furthermore, the addition of nonsialylated LacNAc, but not sucrose, substantially reduced Glut-2-Galectin-9/UAT crosslinking. Together, these findings imply that pancreatic β cell GnT-4a glycosylation of Glut-2 produces an N-glycan ligand for multiple lectins, including Galectin-9/UAT, that reduces the rate of Glut-2 endocytosis and thereby sustains the primary GSIS response.

DISCUSSION

Protein glycosylation by the Golgi-resident GnT-4a glycosyltransferase produces a posttranslational modification on multiple pancreatic glycoproteins that is nevertheless selective in sustaining β cell-surface expression of Glut-2 and thereby maintaining the primary GSIS response. Genetic deficiency of GnT-4a did not affect Glut-2 glycoprotein maturation but reduced Glut-2 cell-surface half-life coincident with endocytosis and accumulation in early endosomes and lysosomes. Similar misglycosylation of other β cell glycoproteins, including the insulin receptor α subunit and the insulin-like growth factor 1 receptor, did not affect total or cell-surface expression. It is therefore in the context of Glut-2 protein sequence that the LacNAc-bearing N-glycan branch contributed by GnT-4a comprises a ligand for endogenous lectin-receptor binding that decreases the rate of endocytosis at the β cell surface. Consistent with the disruption of this lectin binding, loss of β cell-surface Glut-2 expression occurred among wild-type pancreatic islets by the addition of nonsialylated LacNAc-bearing glycan-ligand mimetics. Lectins that may be responsible include Galectin-9/UAT, which colocalizes with and crosslinks to ~40% of total β cell Glut-2 in the presence of wild-type GnT-4a activity. Nevertheless, a molecular accounting for the vast majority of β cell-surface Glut-2 retention likely encompasses other binding partners.

The high-fat diet attenuated pancreatic *Mgat4a* RNA abundance among wild-type C57BL/6 mice coincident with reduced GnT-4a glycosylation of β cell Glut-2. This was associated with diminished cell-surface Glut-2 expression and increased intracellular localization in early endosomes and lysosomes, similar to findings among *Mgat4a* null mice inherently lacking GnT-4a activity. When provided to various rodent strains, the high-fat diet evokes a robust model of type 2 diabetes with loss of GSIS leading to hyperglycemia throughout the diet, while circulating insulin levels are initially decreased but progressively increase over time (Surwit et al., 1988; Winzell and Ahren, 2004). Within 8

(J) In vitro GSIS measured by perfusion performed twice in parallel with identical results using 2×10^5 isolated islet cells from wild-type (white circles) and *Mgat4a* null (black circles) littermates. The glucose concentration of the perfusate was increased from 2.8 mM to 16.8 mM at 4 min.

(K) Time course of glucose analog 2-NBDG uptake (500 mM extracellular concentration) by wild-type islet cells in the absence (white circles) and presence (white squares) of 10 mM nonlabeled D-glucose and by *Mgat4a* null islet cells (black circles). Fluorescence intensities are expressed as relative fluorescence units (RFU). Data are represented as the means \pm SEM from three experiments ($p = 0.0001$).

(L) Lineweaver-Burke plot of 2-NBDG uptake by islet cells from wild-type (white circles) and *Mgat4a* null (black circles) littermates. The K_d value for wild-type and *Mgat4a* null islet cells are 9.525 and 9.104 mM, respectively. V_{max} values in nmol/5 min/ 0.5×10^5 cells are 16.95 for wild-type islets and 1.86 for *Mgat4a* null islets. All mice used in these studies were 8–12 weeks of age except for those analyzed in (G), (H), and (I), as indicated.

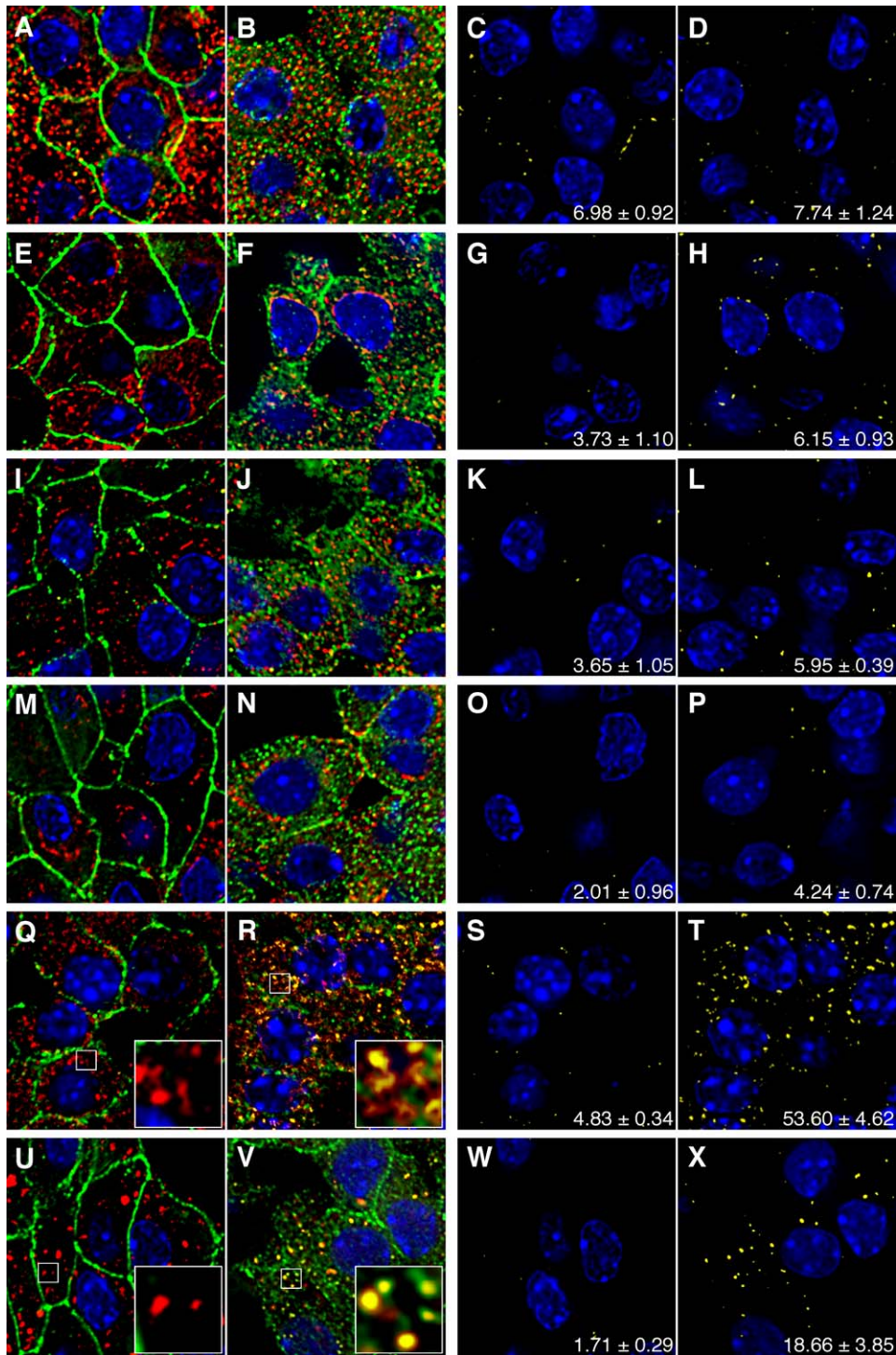


Figure 3. In Situ Localization of Glut-2 in Wild-Type and *Mgat4a* Null Pancreatic β Cells

Pancreatic islet sections of 12-week-old wild-type mice (A, C, E, G, I, K, M, O, Q, S, U, W) and *Mgat4a* null littermates (B, D, F, H, J, L, N, P, R, T, V, X) fed a standard chow diet ad libitum were analyzed by fluorescence deconvolution microscopy for β cell Glut-2 (green) and various intracellular compartments (red), including secretory vesicular insulin (A–D), endoplasmic reticulum protein disulfide isomerase (E–H), *cis*-Golgi Calnuc (I–L), *trans*-Golgi adaptin γ (M–P), early endosome antigen EEA-1 (Q–T), and lysosome LAMP2 (U–X). Colocalization (yellow) of Glut-2 with each of these markers is depicted in separate panels (C, D, G, H, K, L, O, P, S, T, W, X). DNA is stained by DAPI (blue). Inset boxes have been enlarged to enhance visualization of early endosome or lysosome signals. The percentage of Glut-2 colocalization with the relevant cellular marker is indicated in white numbers.

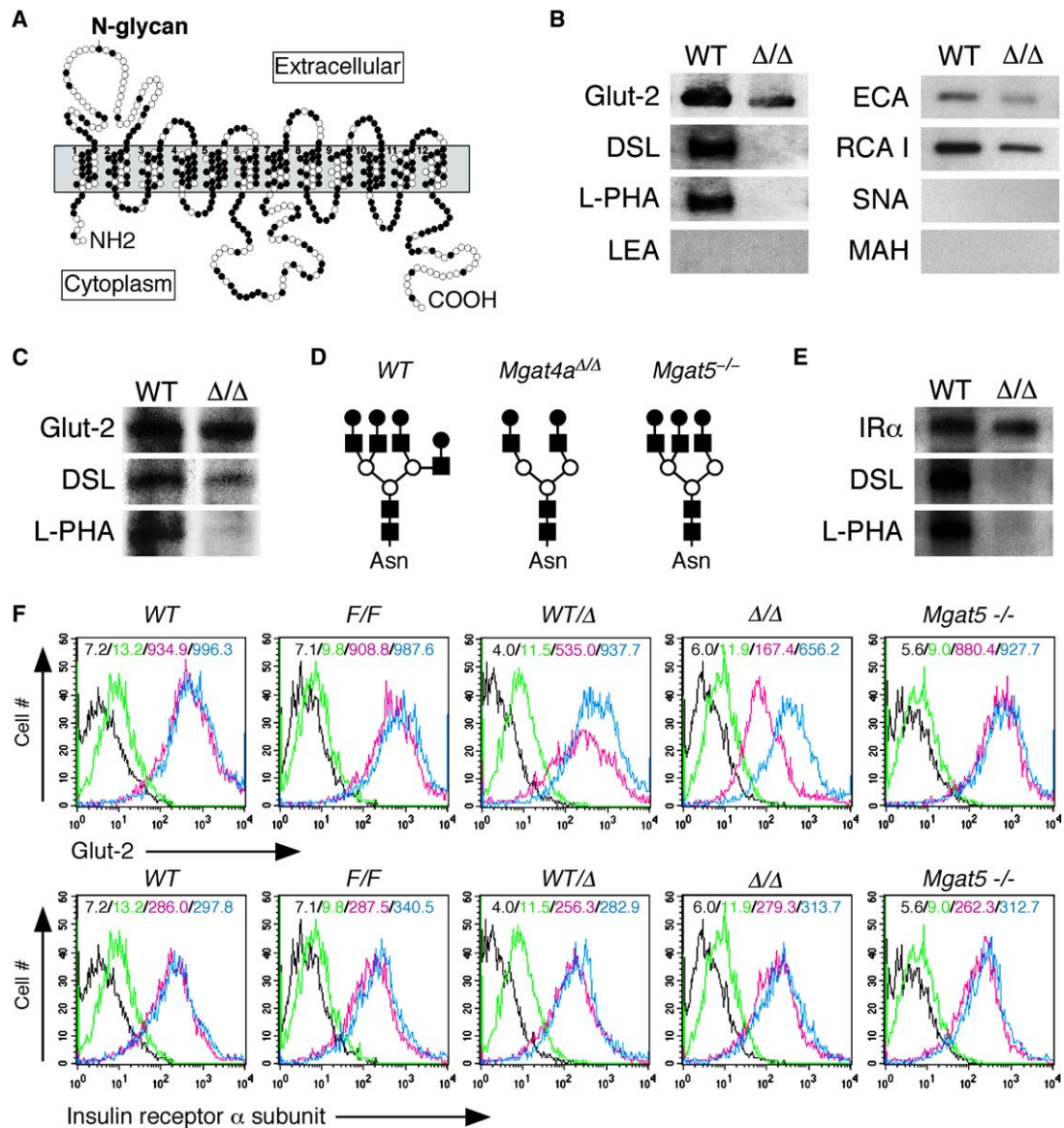


Figure 4. Glut-2 Glucose-Transporter Structure, Glycosylation, and Expression

(A) Conservation and predicted topology of vertebrate Glut-2 orthologs. The orientation of Glut-2 in the lipid bilayer was proposed from its homology to Glut-1 and Glut-4 and by the hydropathy plot of its amino acid sequence (modified from Olson and Pessin, 1996). A single N-glycosylation site is conserved in the first large extracellular domain of Glut-2. Black and white circles indicate identical or nonidentical amino acids, respectively, among human, rat, and chicken orthologs compared to the mouse Glut-2 sequence.

(B) Pancreatic islet Glut-2 abundance and lectin binding analysis of Glut-2 N-glycan structure in wild-type and *Mgat4a* null littermates.

(C) Pancreatic islet Glut-2 abundance and lectin blot analysis of N-glycan structure in wild-type and *Mgat5* null littermates.

(D) Pancreatic Glut-2 N-glycan structures inferred from lectin binding profiles among wild-type, *Mgat4a* null, and *Mgat5* null islet cells.

(E) Abundance and lectin binding analysis of N-glycan structures of insulin receptor α chain in pancreatic islet cells of wild-type and *Mgat4a* null littermates.

(F) Flow cytometric analysis of pancreatic islet cells for Glut-2 or insulin receptor α subunit expression. Cell autofluorescence (black), secondary antibody nonspecific binding (green), cell-surface expression (red), and total (membrane-permeable) cell expression (blue) are plotted. Mean fluorescence level is indicated in each histogram.

weeks on the high-fat diet, intracellular Glut-2 accumulation occurs with loss of the first phase of GSIS, recapitulating the early diabetic pathology in GnT-4a-deficient mice (Reimer and Ahren, 2002). These findings are consistent with the possibility that the pathogenesis of type 2 diabetes in-

response to a high-fat diet may be contingent upon diminished cell-surface Glut-2 levels due to reduced GnT-4a activity.

Attenuated glucose-transporter expression and loss of GSIS are characteristic of early pancreatic β cell dysfunction in multiple manifestations of type 2 diabetes among

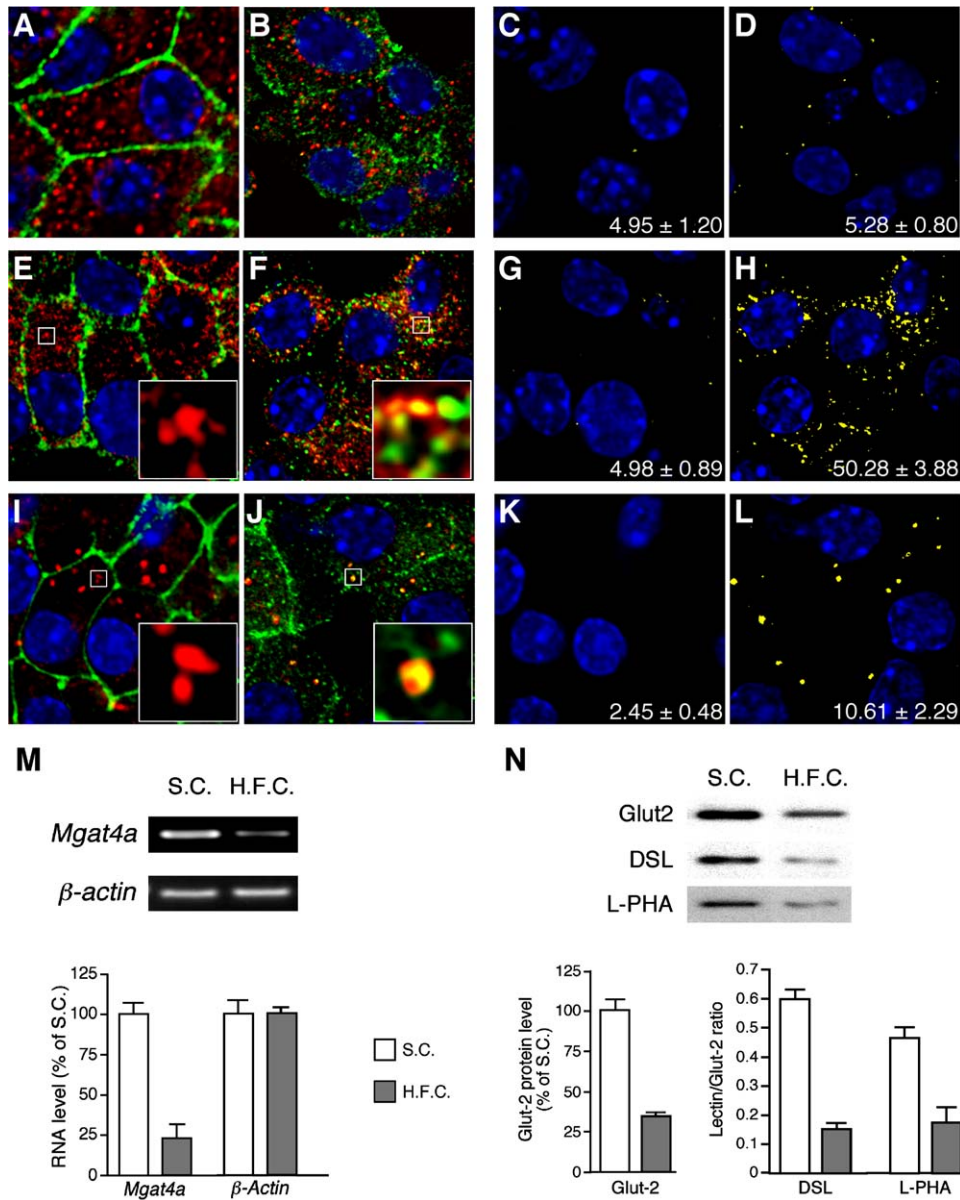


Figure 5. Dietary Regulation of GnT-4a Expression Is Associated with Altered Glut-2 Glycosylation and Trafficking

Pancreatic islet sections of 3-month-old wild-type mice fed ad libitum a standard diet (A, C, E, G, I, K) or a high-fat diet for 8 weeks (B, D, F, H, J, L) were analyzed by fluorescence deconvolution microscopy for β cell Glut-2 expression (green) and various intracellular compartments (red), including insulin-bearing secretory vesicles (A and B), early endosomes (E and F), or lysosomes (I and J). Colocalization (yellow) of Glut-2 with each these markers is shown in separate panels (C, D, G, H, K, L). DNA is stained by DAPI (blue). Inset boxes have been enlarged to enhance visualization of early endosome or lysosome signals. The percentage of Glut-2 colocalization with the relevant cellular marker is indicated in white numbers.

(M) Pancreatic islet *Mgat4a* and β -actin RNA levels from 4-month-old wild-type mice fed ad libitum either a standard chow diet or a high-fat diet for 8 weeks. Total RNA was used for ERT-PCR. Amplified products were quantified by ^{32}P incorporation and graphed as a percentage of RNA abundance compared to littermates fed the standard chow diet.

(N) Glut-2 expression and N-glycosylation among islets of wild-type mice treated as above. The absolute integrated optical density (IOD) of each band was measured and tabulated as either total Glut-2 protein expression (left) or ratios of lectin binding to Glut-2 protein levels (right). Data in (M) and (N) are plotted as means \pm SEM.

humans and rodents, including Zucker diabetic fatty rats, bio-breeding/Worcester diabetic rats, and *db/db* mice lacking the leptin receptor (Orci et al., 1990b; Thorens, et al., 1990, 1992; Unger, 1991; Guerra et al., 2005). It is not known

whether these diabetic conditions are also associated with a similar deficit of Glut-2 N-glycosylation due to diminished GnT-4a expression. Nevertheless, the influence of Glut-2 expression in pathogenesis is known from genetic studies in

the mouse in which β cells bearing 20% or less of normal Glut-2 levels lacked the primary GSIS response and developed type 2 diabetes signs, similar to GnT-4a deficiency (see Table S1 in the Supplemental Data available with this article online). This pathogenic route evoked by β cell failure initially leads to hyperglycemia and insulin insufficiency. Elevations in liver gluconeogenesis and circulating free fatty acids further result, and hepatic steatosis subsequently develops while hyperinsulinemia occurs from compensatory and secondary GSIS secretion mechanisms. The insulin resistance observed in aging GnT-4a-deficient mice likely reflects gluco- and lipotoxicity among muscle and liver tissue.

Altered glycosylation of glucose transporters may be involved in the pathogenesis of human diabetes. However, this may not arise from mutations identified in glucose-transporter protein sequences, which thus far do not alter the N-glycosylation consensus site. *MGAT4A* and *MGAT4B* genes encoding the human GnT-4 isozymes reside at chromosomal positions 2q11-12 and 5q35, respectively, regions of linkage to recently identified type 2 diabetes susceptibility loci (McCarthy, 2003; Reynisdottir et al., 2003; Van Tilburg et al., 2003). Moreover, the predicted promoter sequence of *Mgat4a* contains DNA binding sites for transcriptional factors that are mutated in human mature onset diabetes of the young, also termed MODY. Additionally, an alteration in the repertoire of glycosyltransferase expression among β cells may also cause diabetes by a dominant genetic mechanism. For example, pancreatic Glut-2 N-glycan structures appear deficient in terminal sialic-acid linkages, while sialylated LacNAc N-glycans failed to induce Glut-2 endocytosis. Hence, a mutational event that induced sialic-acid linkage formation on the Glut-2 N-glycan would likely mask the lectin ligand and thereby attenuate cell-surface Glut-2 expression.

The coordinated expression patterns of glycosyltransferases and proteins in the secretory pathway among diverse cell types generate posttranslational modifications that operate as regulatory elements in metabolism and disease. Nevertheless, our findings imply that a proportion of protein glycosylation attributed to any one glycosyltransferase such as GnT-4a may be physiologically inert. This may reflect the absence of a selective advantage in eliminating innocuous posttranslational protein modifications in evolution or perhaps an inherent value of such structural variation in evolving protein function. While a specific glycan linkage may structurally if not functionally modify many proteins, this combinatorial assortment permits the formation of unique glycoprotein configurations that, in some contexts, comprise ligands for endogenous lectin receptors. Pancreatic β cell N-glycosylation of Glut-2 in the Golgi apparatus by the GnT-4a glycosyltransferase appears to produce such a lectin-receptor ligand that, in *cis* and perhaps in *trans*, is essential for Glut-2 retention at the cell surface. The specificity of GnT-4a function further appears to be cell type specific. No expression of GnT-4 activity or associated N-glycan branching could be demonstrated in hepatocytes, and hepatic Glut-2 cell-surface expression was unaltered by GnT-4a deficiency (Figure S1). Glut-2 N-glycan structures in the liver appear to be heterogenic biantennary-complex-type forms bearing terminal gal-

lactose and sialic-acid linkages among both wild-type and GnT-4a-deficient mice. Therefore, the mechanistic features comprising cell-type-specific control of Glut-2 endocytosis by GnT-4a glycosylation likely involve a specialized infrastructure in pancreatic β cells that engages membrane cytoskeletal and scaffolding proteins. Further identifying the molecular nature of dietary and genetic factors that influence GnT-4a expression will reveal additional components of this mechanism and perhaps a rationale for its disengagement in response to the high-fat diet. Should enforced β cell GnT-4 expression enhance Glut-2 cell-surface levels, it may be possible to intervene in the early pancreatic dysfunction associated with the loss of GSIS that is a harbinger of further metabolic alterations to follow in the pathogenesis of type 2 diabetes.

EXPERIMENTAL PROCEDURES

Mgat4a Expression and Mutagenesis

Mouse *Mgat4a* cDNA clones GT4F7/GT4R6 and GT4F3/GB5 were obtained by RT-PCR and used as probes to isolate an 11 kb *Mgat4a* clone from a 129/SvJ genomic DNA bacteriophage library (Stratagene, San Diego, CA). Chimeric mice were generated from C57BL/6 blastocyst-stage embryos and ES cells bearing the conditional (F, type 2) *Mgat4a* mutation (Figures 1C and 1D). Female mice bearing a germline *Mgat4a^F* allele and the Zp3-Cre transgene (Shafi et al., 2000) were bred to acquire offspring containing the *Mgat4a^d* allele. In RNA expression analyses using a mouse *Mgat4a* cDNA probe (nt 181–339), total RNA was subjected to 1% formaldehyde-denaturing agarose gel electrophoresis.

Mouse Breeding and Maintenance

The *Mgat4a^d* and *Mgat4a^F* alleles were bred into the C57BL/6 background at least six generations prior to producing offspring for study. Mice lacking GnT-5 (Demetriou et al., 2001) were provided by James Dennis (Toronto). Mice were housed in specific-pathogen-free conditions and provided either a standard chow diet (16.4% protein, 73.1% carbohydrates, and 10.5% fat with 4.07 kcal/g [D12329, Research Diets, New Brunswick, NJ]) or a high-fat chow diet (16.4% protein, 25.5% carbohydrates, and 58.0% fat with 5.56 kcal/g [D12331, Research Diets]).

GnT-4 Enzymology

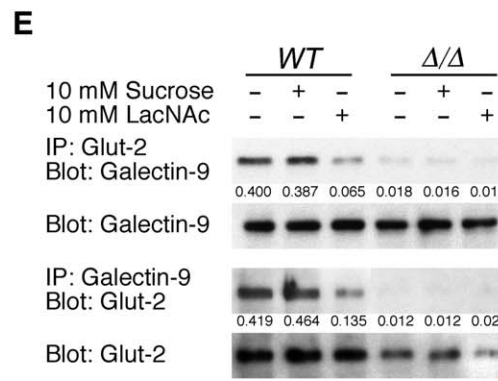
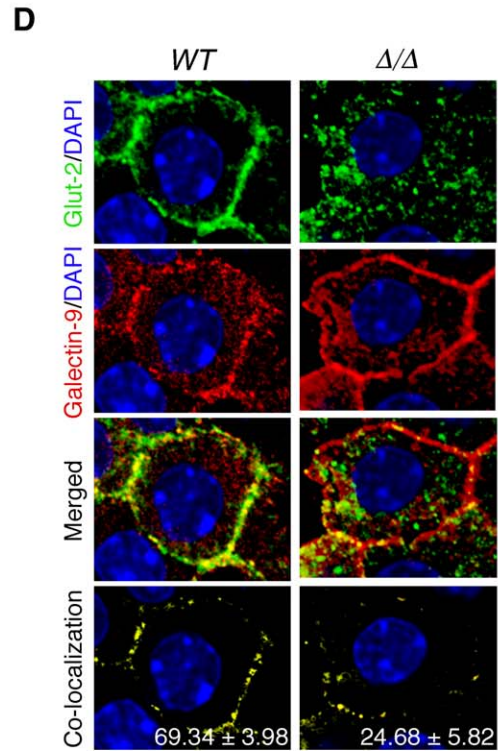
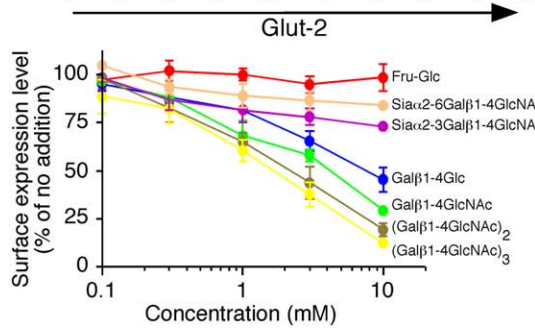
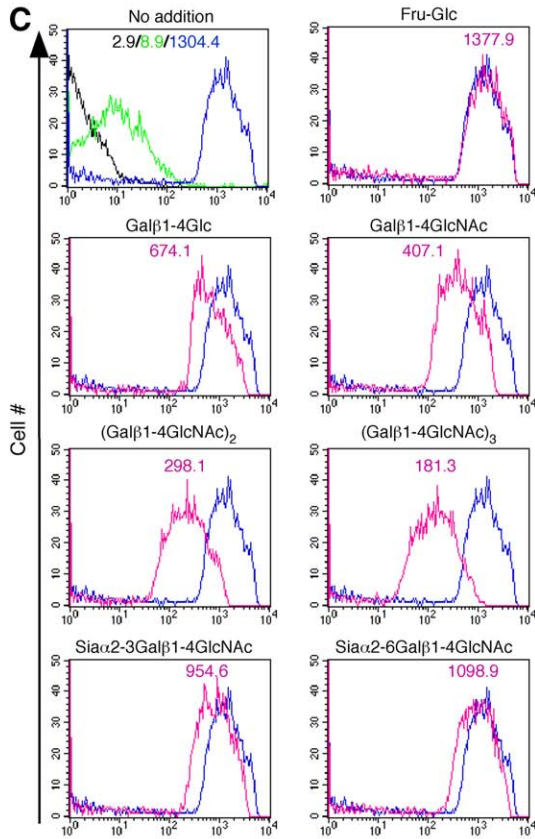
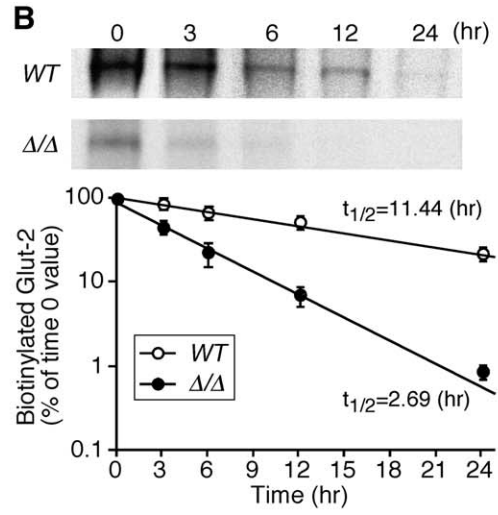
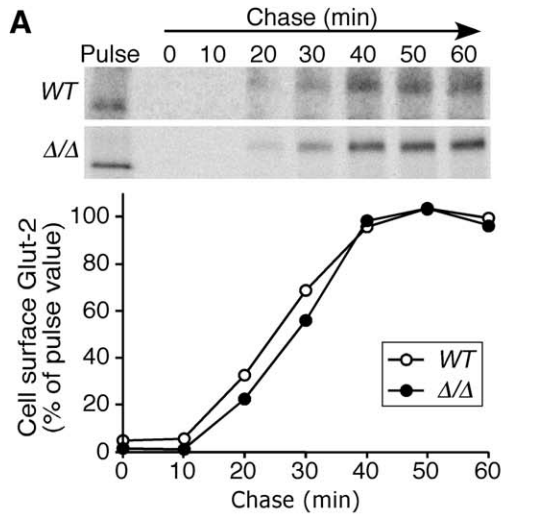
GnT-4 activity was measured in tissue homogenates by reverse-phase HPLC in a modification of previous methods (Oguri et al., 1997). The substrate GlcNAc β 1-2Man α 1-6(GlcNAc β 1-2Man α 1-3) Man β 1-4GlcNAc β 1-4GlcNAc β 1-2-aminopyridine was prepared as described (Tokugawa et al., 1996).

Serum Chemistry

Blood was collected in the absence of anticoagulants by orbital sinus bleed or cardiac puncture and was allowed to clot in a serum separator tube in which the serum was collected by centrifugation (Becton Dickinson, Mountain View, CA). Blood-chemistry analysis was performed using a Beckman CX-7 automated analyzer with a general coefficient of variation of <5%.

Histology and Microscopy

For determining pancreatic morphology and islet abundance, 3 μ m pancreatic tissue sections were stained with anti-insulin antibody (Linco Research, St. Charles, MO) followed by secondary horseradish peroxidase (HRP) conjugated anti-guinea pig antibody (ICN Biomedicals, Irvine, CA) and visualized using ABC staining (Vector, Burlingame, CA). Cell nuclei were counterstained with hematoxylin. Islet cross-sectional areas were measured using KS300 software (Carl Zeiss, Jena, Germany). For immunofluorescence analyses of pancreatic islets, tissue sections were



incubated with Glut-2 antibody (Chemicon, Temecula, CA) combined with antibodies to either insulin, PDI (Stressgen, Victoria, Canada), Calnuc (a gift from Marilyn G. Farquhar, University of California, San Diego, CA), adaptin γ (BD Transduction Laboratories, San Diego, CA), EEA1 (BD Transduction Laboratories), or LAMP2 (Santa Cruz Biotechnology, Santa Cruz, CA) at 1:200 dilution. Glut-2 was visualized using FITC-conjugated sheep anti-rabbit IgG (ICN Biomedicals). PDI, adaptin γ , EEA1, and LAMP2 were visualized with rhodamine-conjugated goat anti-mouse IgG (ICN Biomedicals). Calnuc was visualized with rhodamine-conjugated goat anti-chicken IgY (Molecular Probes, Eugene, OR). Insulin was visualized with rhodamine-conjugated goat anti-guinea pig IgG (ICN Biomedicals). Cryostat-sectioned (3 μ m) liver was stained with hematoxylin and eosin or Nile blue. Galectin-9 antibodies (M20, Santa Cruz Biotechnology) were used with rhodamine-conjugated donkey anti-goat IgG (Molecular Probes). Images were analyzed by deconvolution using a Delta Vision Restoration microscope (Applied Precision Inc., Issaquah, WA) and Delta Vision SoftWork software (Version 2.50). Colocalization was quantified by object-based analysis at multiple exclusion thresholds spanning the linear range of fluorescent signals using MetaMorph algorithms (Universal Imaging Corporation, Downingtown, PA).

Glucose and Insulin Homeostasis

Mice were fasted for 16 hr followed by intraperitoneal glucose injection (1.5 g/kg body weight). Serum samples were obtained at 0, 30, 60, 120, and 240 min after the injection, and measurements of glucose and insulin were determined, the latter using a rat insulin ELISA assay with a mouse insulin standard (Crystal Chem, Chicago). In testing insulin tolerance, intraperitoneal injections of 2 U/kg body weight of human insulin (Calbiochem, La Jolla, CA) were performed. In arginine-tolerance tests, mice were fasted for 16 hr followed by intraperitoneal injection (3 g/kg body weight) of L-arginine (Sigma, St. Louis).

Islet Cell Preparation, Culture, and In Vitro Insulin Secretion Assay

Mouse islet cells were obtained as described (Josefsen et al., 1996) and cultured in β cell media containing RPMI-1640 with 10% FCS, 2 mM L-glutamine, 0.1 mM 2-mercaptoethanol, and 11 mM glucose. In the perfusion assay, 2×10^5 islet cells were preincubated in HEPES-buffered Krebs-Ringer bicarbonate solution (KRBH) (10 mM HEPES [pH 7.4], 129 mM NaCl, 4.7 mM KCl, 1.2 mM KH_2PO_4 , 1.2 mM MgSO_4 , 2 mM CaCl_2 , 5 mM NaHCO_3 , and 0.1% BSA) containing 2.8 mM glucose for 30 min at 37°C, then placed in a 0.2 μ m syringe filter (Sartorius). The filter was connected to a peristaltic pump for which the flow rate was adjusted to 1 ml/min and equilibrated with KRBH containing 2.8 mM glucose for 10 min before increasing the glucose concentration to 16.8 mM. Fractions were collected and insulin was quantified by ELISA.

Flow Cytometry

Isolated islet cells were analyzed by flow cytometry with antibodies to Glut-2 (Chemicon) and the insulin receptor α subunit (Santa Cruz Biotechnology) and were found to be between 90% and 95% pancreatic β cells.

Cultured islet cells (24 hr) were harvested with ice-cold 2 mM EDTA in PBS and washed with ice-cold FACS buffer (2% FCS in PBS). Cell membranes were rendered permeable using BD Cytotix/Cytoperm solution for 20 min at 4°C, followed by washing cells twice with Perm/Wash solution (BD Biosciences Pharmingen, San Diego, CA). In analyzing the effects of synthetic glycans, islet cells were cultured in FACS buffer with various glycan concentrations for 2 hr at 37°C. Cell labeling by antibody binding was subsequently carried out in 100 μ l with 50,000 cells in FACS buffer on ice for 10 min. Data were acquired using a FACSCalibur Flow Cytometer and analyzed by CellQuest Software (Becton Dickinson). Antibodies to Glut-2 (Chemicon) and the insulin receptor α subunit (Santa Cruz Biotechnology) were used with FITC-conjugated sheep anti-rabbit IgG at 1.0 μ g/ml and 0.5 μ g/ml, respectively.

Islet Cell Glucose Transport

Glucose transport was measured using 2-[N-(7-nitrobenz-2-oxa-1,3-diazol-4-yl)amino]-2-deoxy-D-glucose (2-NBDG, Molecular Probes) as described (Yamada et al., 2000). Islet cells were incubated in glucose-free-KRBH for 20 min at 37°C and then with various concentrations of 2-NBDG. To measure the time course of 2-NBDG transport, islet cells were incubated with 500 μ M of 2-NBDG in KRBH in the presence or absence of 10 mM D-glucose for the indicated times, then washed three times with glucose free-KRBH, and intracellular fluorescence (excitation 485–495 nm, emission 515–525 nm) was measured using a Versa-Fluor Fluorometer (Bio-Rad, Hercules, CA). Concentration dependence was determined using identical conditions and either 100 μ M, 200 μ M, 400 μ M, 800 μ M, 1.6 mM, 3.2 mM, or 6.4 mM 2-NBDG for 5 min.

mRNA Quantitation

Total RNA (1 μ g) was subjected to reverse transcription using the Super-Script III first-strand synthesis system (Invitrogen). The transcripts were amplified by PCR in the presence of 10 μ Ci of [α - 32 P]dATP (3000 Ci/mmol; PerkinElmer Life and Analytical Sciences, Boston) in 30 μ l of reaction mixture containing primers for *PEPCK* (sense, 5'-ATGCCTCCTCAGCTGCA TAA-3'; antisense, 5'-GAACCTGGCGTTGAATGCTT-3'), *G6Pase* (sense, 5'-AGTCGACTGCTATCTCCAA-3'; antisense, 5'-ACCGGAATCCATA CGTTGGC-3'), *Mgat4a* (sense, 5'-TGAAGCCATTGCTTCTCAAGGTCC-3'; antisense, 5'-GGCCCAACAGCTGAGTTCTGAAT-3'), or β -*actin* (sense, 5'-CGTAAAGACCTCTATGCCAA-3'; antisense, 5'-GGGATGTTTGCTC CAACCAA-3'). The cycle number was set in the linear amplification range (19 to 24 cycles). The relative amount of product was measured as the incorporated 32 P by liquid scintillation counting.

Immunoprecipitation and Glycan Analysis

Isolated islets were suspended in lysis buffer containing 50 mM Tris-HCl (pH 7.5), 150 mM NaCl, 1.2% Triton X-100, 0.05% SDS, and proteinase inhibitor cocktail (Roche, Mannheim, Germany) and sonicated. Solubilized proteins were recovered in supernatants following a 15 min centrifugation at 13,000 rpm in a tabletop centrifuge at 4°C. Total protein (200 μ g) was subjected to immunoprecipitation with antibody to the C-terminal

Figure 6. GnT-4a Glycosylation Promotes Glut-2 Stability at the Cell Surface by a Lectin-Receptor Binding Mechanism

(A) Production and trafficking of newly synthesized Glut-2 in pancreatic islet cells are normal in GnT-4a deficiency. Thirty-five mice of each genotype were analyzed.

(B) Glut-2 cell-surface half-life on intact islet cells was measured following cell-surface biotinylation, then graphed as a percentage of biotinylated Glut-2 present immediately after biotinylation. Data are represented as the means \pm SD from three separate experiments.

(C) Glut-2 expression on the surface of wild-type pancreatic islet cells was monitored by flow cytometry following a 2 hr incubation period with various concentrations of indicated glycan structures. Top panels: plots of cell autofluorescence (black), secondary antibody binding (green), cell-surface expression with no addition (blue), and cell-surface expression with addition of indicated glycan at 10 mM (red). Mean fluorescence level is indicated in matching colored text. Bottom panel: in a dose-response analysis, only LacNAc-bearing N-glycans lacking sialic-acid termini significantly reduced Glut-2 cell-surface expression. Data are plotted as means \pm SEM of triplicate measurements representing one of three separate littermate cell comparisons.

(D) Pancreatic islet sections of 3-month-old wild-type mice and *Mgat4a* null littermates fed a standard chow diet ad libitum were analyzed by fluorescence deconvolution microscopy for Glut-2 expression (green) and Galectin-9/UAT (red). Colocalization (yellow) is presented in separate panels. The percentage of Glut-2 colocalization with Galectin-9/UAT is indicated.

(E) Glut-2 association with Galectin-9/UAT at the pancreatic islet cell surface was assayed by protein crosslinking. Incubation of islet cells at 4°C in the presence of 10 mM of LacNAc (Gal β 1-4GlcNAc), but not sucrose, diminished Glut-2 crosslinking to Galectin-9/UAT. The amount of protein coprecipitated is indicated as a percentage of the total detected.

region of Glut-2 (Santa Cruz Biotechnology). The precipitates were analyzed by blotting with antibody to Glut-2 (Chemicon) or lectins DSL, L-PHA, LEA, ECA, RCA-1, SNA, or MAH (Vector Laboratories). In using biotinylated DSL and L-PHA, blots were rinsed with TBS and incubated with 20 mU/ml of neuraminidase (*Vibrio cholerae*, Sigma) in 50 mM sodium-acetate buffer (pH 5.5) at 37°C for 16 hr, then treated with 125 mU/ml of endo- β -galactosidase (*Escherichia freundii*, Calbiochem) in 50 mM sodium-acetate buffer (pH 5.5) at 37°C for 16 hr. After washing with T-TBS (0.05% Tween 20 in TBS), blots were incubated with 5% BSA in T-TBS followed by 2 mg/ml of either DSL or L-PHA in T-TBS with 1% BSA. After incubating with HRP-streptavidin (BD Pharmingen), blots were washed and developed by enhanced chemiluminescence (Amersham Biosciences, Buckinghamshire, England). For quantifying signals, the absolute integrated optical density (IOD) was measured using Labworks software (UVP Bioimaging Systems, Upland, CA).

Pulse-Chase Analysis, Cell-Surface Half-Life, and Protein Crosslinking

Islet cells were washed twice with HBSS, then incubated with RPMI 1640 medium depleted of methionine (Sigma) with 10% dialyzed fetal calf serum (GIBCO/Invitrogen, Carlsbad, CA) for 2 hr at 37°C. Pulse labeling was performed with 400 μ Ci/ml [³⁵S]methionine for 10 min at 37°C, and cells were then washed twice in ice-cold HBSS. Cells were lysed or returned to above culture conditions containing 2 mM methionine for 10, 20, 30, 40, 50, or 60 min. Cells used in chase samples were washed twice with ice-cold PBS and incubated with 1 mg/ml of sulfo-NHS-LC-biotin (Pierce Chemical, Rockford, IL) at 4°C for 30 min. Biotinylation was stopped by three washes with 15 mM glycine in ice-cold PBS. Cells were homogenized in lysis buffer, and biotinylated proteins were purified using immobilized monomeric avidin gel (Pierce Chemical). Eluates isolated in the presence of D-biotin (Pierce Chemical) were incubated with anti-Glut-2 C-terminal antibody. Immunoprecipitates were subjected to SDS-PAGE, and gels were fixed before drying and autoradiography at -70°C for 3 to 7 days. For cell-surface half-life analysis, islet cells were washed twice with ice-cold PBS and biotinylated with sulfo-NHS-LC-biotin as described above. Cells were further cultured for 3, 6, 12, or 24 hr, then homogenized in lysis buffer, followed by immunoprecipitation using the anti-Glut-2 C-terminal antibody. Glut-2 immunoprecipitates were visualized with HRP-conjugated streptavidin. For cell-surface protein crosslinking, islet cells were washed twice with HBSS and then incubated with synthetic glycans in RPMI 1640 medium for 2 hr at 4°C. Cells were washed twice with ice-cold PBS, then incubated with 2 mM dithio-bis-sulfosuccinimidypropionate in PBS for 2 hr on ice. Crosslinking was terminated by the addition of 1 M Tris-HCl (pH 7.5) to a final concentration of 10 mM. Cells were then homogenized in lysis buffer, and Glut-2 or Galectin-9 was precipitated using antibodies to the C-terminal residues of Glut-2 or Galectin-9.

Statistical Analysis

Data were plotted as the mean of the number (n) of samples analyzed \pm the standard error unless otherwise indicated. Student's t test was used to calculate indicated p values.

Supplemental Data

Supplemental Data include Supplemental References, one table, and one figure and can be found with this article online at <http://www.cell.com/cgi/content/full/123/7/1307/DC1/>.

ACKNOWLEDGMENTS

We thank Marilyn Farquhar and Jerrold Olefsky for helpful discussions and critical comments. Glycan compounds were provided by Ola Blixt and the Consortium for Functional Glycomics (NIH GM62116). Deconvolution microscopy was accomplished at the UCSD Cancer Center Digital Imaging Shared Resource laboratory, directed by Dr. James Feramisco. This research was funded by NIH grant DK48247 and an Investigator award from the Howard Hughes Medical Institute (J.D.M.). The remaining

coauthors wish to dedicate this manuscript to the life and career of Makoto Takeuchi, who died on November 29, 2001.

Received: July 11, 2005

Revised: August 29, 2005

Accepted: September 20, 2005

Published: December 28, 2005

REFERENCES

- Asano, T., Takata, K., Katagiri, H., Ishihara, H., Inukai, K., Anai, M., Hirano, H., Yazaki, Y., and Oka, Y. (1993). The role of N-glycosylation in the targeting and stability of GLUT1 glucose transporter. *FEBS Lett.* 324, 258–261.
- Cooper, D.N., and Barondes, S.H. (1999). God must love galectins; he made so many of them. *Glycobiology* 9, 979–984.
- Cummings, R.D. (1999). Plant lectins. In *Essentials of Glycobiology*, A. Varki, R. Cummings, J. Esko, H. Freeze, G. Hart, and J. Marth, eds. (Cold Spring Harbor, NY: Cold Spring Harbor Laboratory Press), pp. 455–467.
- Demetriou, M., Granovsky, M., Quaggin, S., and Dennis, J. (2001). Negative regulation of T-cell activation and autoimmunity by Mgat5 N-glycosylation. *Nature* 409, 733–739.
- Gremlich, S., Roduit, R., and Thorens, B. (1997). Dexamethasone induces posttranslational degradation of GLUT2 and inhibition of insulin secretion in isolated pancreatic β cells. *J. Biol. Chem.* 272, 3216–3222.
- Guerra, S.D., Lupi, R., Marselli, L., Masini, M., Bugliani, M., Sbrana, S., Torri, S., Pollera, M., Boggi, U., Mosca, F., et al. (2005). Functional and molecular defects of pancreatic islets in human type 2 diabetes. *Diabetes* 54, 727–735.
- Guillam, M.T., Hümmeler, E., Schaerer, E., Wu, J.-Y., Birnbaum, M.J., Beermann, F., Schmidt, A., Dériaz, N., and Thorens, B. (1997). Early diabetes and abnormal postnatal pancreatic islet development in mice lacking Glut-2. *Nat. Genet.* 17, 327–330.
- Guillam, M.T., Dupraz, P., and Thorens, B. (2000). Glucose uptake, utilization, and signaling in GLUT2-null islets. *Diabetes* 49, 1485–1491.
- Ing, B.L., Chen, H., Robinson, K.A., Buse, M.G., and Quon, M.J. (1996). Characterization of a mutant Glut-4 lacking the N-glycosylation site: Studies in transfected rat adipose cells. *Biochem. Biophys. Res. Commun.* 218, 76–82.
- Johnson, J.H., Ogawa, A., Chen, L., Orci, L., Newgard, C.B., Alam, T., and Unger, R.H. (1990). Underexpression of beta cell high Km glucose transporters in noninsulin-dependent diabetes. *Science* 250, 546–549.
- Joost, H.G., and Thorens, B. (2001). The extended GLUT-family of sugar/polyol transport facilitators: nomenclature, sequence characteristics, and potential function of its novel members (review). *Mol. Membr. Biol.* 18, 247–256.
- Josefsen, K., Stenvang, J.P., Berggren, P.O., Horn, T., Kjaer, T., and Buschard, K. (1996). Fluorescence-activated cell sorted rat islet cells and studies of the insulin secretory process. *J. Endocrinol.* 149, 145–154.
- Lee, S.K., Opara, E.C., Surwit, R.S., Feinglos, M.N., and Akwari, O.E. (1995). Defective glucose-stimulated insulin release from perfused islets of C57BL/6J mice. *Pancreas* 11, 206–211.
- Lipkowitz, M.S., Leal-Pinto, E., Cohen, B.E., and Abramson, R.G. (2004). Galectin 9 is the sugar-regulated urate transporter/channel UAT. *Glycoconj. J.* 19, 491–498.
- Lowe, J.B., and Marth, J.D. (2003). A genetic approach to mammalian glycan function. *Annu. Rev. Biochem.* 72, 673–691.
- Macheda, M.L., Rogers, S., and Best, J.D. (2005). Molecular and cellular regulation of glucose transporter (GLUT) proteins in cancer. *J. Cell. Physiol.* 202, 654–662.
- McCarthy, M.I. (2003). Growing evidence for diabetes susceptibility genes from genome scan data. *Curr. Diab. Rep.* 3, 159–167.

- Minowa, M.T., Oguri, S., Yoshida, A., Hara, T., Iwamatsu, A., Ikenaga, H., and Takeuchi, M. (1998). cDNA cloning and expression of bovine UDP-N-acetylglucosamine: α 1,3-D-mannoside β 1,4-N-acetylglucosaminyltransferase IV. *J. Biol. Chem.* *273*, 11556–11562.
- Oguri, S., Minowa, M.T., Ihara, Y., Taniguchi, N., Ikenaga, H., and Takeuchi, M. (1997). Purification and characterization of UDP-N-acetylglucosamine: α 1,3-D-mannoside β 1,4-N-acetylglucosaminyltransferase (N-acetylglucosaminyltransferase-IV) from bovine small intestine. *J. Biol. Chem.* *272*, 22721–22727.
- Olson, A.L., and Pessin, J.E. (1996). Structure, function, and regulation of the mammalian facilitative glucose transporter gene family. *Annu. Rev. Nutr.* *16*, 235–256.
- Orci, L., Ravazzola, M., Baetens, D., Inman, L., Amherdt, M., Peterson, R.G., Newgard, C.B., Johnson, J.H., and Unger, R.H. (1990a). Evidence that down-regulation of β -cell glucose transporters in non-insulin-dependent diabetes may be the cause of diabetic hyperglycemia. *Proc. Natl. Acad. Sci. USA* *87*, 9953–9957.
- Orci, L., Unger, R.H., Ravazzola, M., Ogawa, A., Komiya, I., Baetens, D., Lodish, H.F., and Thorens, B. (1990b). Reduced β -cell glucose transporter in new onset diabetic rats. *J. Clin. Invest.* *86*, 1615–1622.
- Reimer, M.K., and Ahren, B. (2002). Altered β -cell distribution of pdx-1 and GLUT2 after a short-term challenge with a high-fat diet in C57BL/6J mice. *Diabetes* *51* Suppl. 1, S138–S143.
- Reynisdottir, I., Thorleifsson, G., Benediktsson, R., Sigurdsson, G., Emilsson, V., Einarsdottir, A.S., Hjorleifsdottir, E.E., Orlygsdottir, G.T., Hrafnkelsdottir, S., Saemundsdottir, S.B., et al. (2003). Localization of a susceptibility gene for type 2 diabetes to chromosome 5q34-q35.2. *Am. J. Hum. Genet.* *73*, 323–335.
- Sato, M., Nishi, N., Shoji, H., Seki, M., Hashidate, T., Hirabayashi, J., Kasai, K., Hata, Y., Suzuki, S., Hirashima, M., et al. (2002). Functional analysis of the carbohydrate recognition domains and a linker peptide of galectin-9 as to eosinophil chemoattractant activity. *Glycobiology* *12*, 191–197.
- Shafi, R., Iyer, S.P.N., Ellies, L.G., O'Donnell, N., Marek, K.W., Chui, D., Hart, G.W., and Marth, J.D. (2000). The O-GlcNAc transferase gene resides on the X chromosome and is essential for embryonic stem cell viability and mouse ontogeny. *Proc. Natl. Acad. Sci. USA* *97*, 5735–5739.
- Surwit, R.S., Kuhn, C.M., Cochrane, C., McCubbin, J.A., and Feinglos, M.N. (1988). Diet-induced type II diabetes in C57BL/6J mice. *Diabetes* *37*, 1163–1167.
- Thorens, B., Weir, G., Leahy, J.L., Lodish, H.F., and Bonner-Weir, S. (1990). Reduced expression of the liver/ β -cell glucose transporter isoform in glucose-insensitive pancreatic β cells of diabetic rats. *Proc. Natl. Acad. Sci. USA* *87*, 6492–6496.
- Thorens, B., Wu, Y.-J., Leahy, J.L., and Weir, G.C. (1992). The loss of GLUT2 expression by glucose-unresponsive β cells of db/db mice is reversible and is induced by the diabetic environment. *J. Clin. Invest.* *90*, 77–85.
- Thorens, B., Gérard, N., and Dériaz, N. (1993). GLUT2 surface expression and intracellular transport via the constitutive pathway in pancreatic β cells and insulinoma: evidence for a block in trans-golgi network exit by brefeldin A. *J. Cell Biol.* *123*, 1687–1694.
- Tokugawa, K., Oguri, S., and Takeuchi, M. (1996). Large scale preparation of PA-oligosaccharides from glycoproteins using an improved extraction method. *Glycoconj. J.* *13*, 53–56.
- Unger, R.H. (1991). Diabetic hyperglycemia: link to impaired glucose transport in pancreatic β cells. *Science* *251*, 1200–1205.
- Valera, A., Solanes, G., Fernández-Alvarez, J., Pujol, A., Ferrer, J., Asins, G., Gomis, R., and Bosch, F. (1994). Expression of GLUT2 antisense RNA in β cells of transgenic mice leads to diabetes. *J. Biol. Chem.* *269*, 28543–28546.
- Van Tilburg, J.H.O., Sandkuij, L.A., Strengman, E., Van Someren, H., Rigters-Aria, C.A.E., Pearson, P.L., Haeflén, T.W., and Wijmenga, C. (2003). A genome-wide scan in type 2 diabetes mellitus provides independent replication of a susceptibility locus on 18p11 and suggests the existence of novel loci on 2q12 and 19q13. *J. Clin. Endocrinol. Metab.* *88*, 2223–2230.
- Winzell, M.S., and Ahren, B. (2004). The high-fat diet-fed mouse: a model for studying mechanisms and treatment of impaired glucose tolerance and type 2 diabetes. *Diabetes* *53* Suppl. 3, S215–S219.
- Yamada, K., Nakata, M., Horimoto, N., Saito, M., Matsuoka, H., and Inagaki, N. (2000). Measurement of glucose uptake and intracellular calcium concentration in single, living pancreatic β -cells. *J. Biol. Chem.* *275*, 22278–22283.
- Yoshida, A., Minowa, M.T., Takamatsu, S., Hara, T., Ikenaga, H., and Takeuchi, M. (1998). A novel second isozyme of the human UDP-N-acetylglucosamine: α 1,3-D-mannoside β 1,4-N-acetylglucosaminyltransferase family: cDNA cloning, expression, and chromosomal assignment. *Glycoconj. J.* *15*, 1115–1123.